Front. Phys. 13(2), 137301 (2018)
https://doi.org/10.1007/s11467-017-0730-6

RESEARCH ARTICLE

Fractal dimension study of polaron effects in cylindrical GaAs/$Al_xGa_{1-x}As$ core–shell nanowires

Hui Sun[1], **Hua Li**[2], **Qiang Tian**[1,†]

[1] *Department of Physics, Beijing Normal University, Beijing 100875, China*
[2] *Department of Fundamental Courses, Academy of Armored Forces Engineering, Beijing 100072, China*
Corresponding author. E-mail: †*qiangtian163@163.com*
Received April 2, 2017; accepted August 28, 2017

Polaron effects in cylindrical GaAs/$Al_xGa_{1-x}As$ core–shell nanowires are studied by applying the fractal dimension method. In this paper, the polaron properties of GaAs/$Al_xGa_{1-x}As$ core–shell nanowires with different core radii and aluminum concentrations are discussed. The polaron binding energy, polaron mass shift, and fractal dimension parameter are numerically determined as functions of shell width. The calculation results reveal that the binding energy and mass shift of the polaron first increase and then decrease as the shell width increases. A maximum value appears at a certain shell width for different aluminum concentrations and a given core radius. By using the fractal dimension method, polaron problems in cylindrical GaAs/$Al_xGa_{1-x}As$ core–shell nanowires are solved in a simple manner that avoids complex and lengthy calculations.

Keywords core–shell nanowire, polaron effects, fractal dimension method

PACS numbers 73.63.-b, 73.90.+f, 73.63.Nm

1 Introduction

Core–shell nanowires are widely regarded as the next frontier in applications to numerous optoelectronic and electronic devices [1–3]. GaAs and $Al_xGa_{1-x}As$ are important materials that are typically used to fabricate these semiconductor nanowires [1–5], and we use the fractal dimension method to explore polaron effects in GaAs/$Al_xGa_{1-x}As$ core–shell nanowires. The polaron properties and fractional dimension parameter are calculated as a function of shell width.

During the past few years, considerable progress has been made on low-dimensional semiconductor systems. Polaron effects have drawn significant research attention. The polaron properties of quantum wells can be studied simply and with good accuracy by using the fractal dimension framework [6–12]. The fractal dimension method proposed by He [6] has been successfully used to study polarons in film quantum wells [7–12]. Recently, the fractal dimension method has been successfully applied to model excitons [13–16], polarons [17], and impurities [18–21] in semiconductor materials. In the fractal dimension method, anisotropic interactions in real space are assumed to be isotropic interactions in an effective fractal dimension environment, the dimension of which measures the degree of anisotropy in the real physical environment. Accordingly, all relevant anisotropic problems can be solved by introducing a single quantity, i.e., the dimension. By considering this quantity, we can model the real physical environment in a simple analyzable way. Polaron problems in heterostructures are very complicated owing to the presence of a variety of phonon modes such as bulklike phonons, interface phonons, half-space phonons, and slab phonons. Smondyrev *et al.* [22] proposed a simplified polaron model in which these effects are taken into account. Polaron problems in multilayered heterostructures can then be solved simply by considering only one bulk phonon mode and the effective confining potential. On the basis of Smondyrev *et al.*'s work, Matos–Abiague [7–9] formulated a simplified model to solve polaron problems in GaAs/$Al_xGa_{1-x}As$ quantum wells by the fractal dimension method. Then the polaron corrections can be calculated by considering only one bulk phonon mode and the fractal dimension. The aim of this paper is to calculate the polaron properties of differently shaped low-dimensional heterostructures using a simple analysis method: the fractal dimension method.

To our knowledge, few studies of core–shell nanowires

consider the polaron properties, especially those of GaAs/Al_xGa_{1-x}As core–shell nanowires consisting of an Al_xGa_{1-x}As core surrounded by a GaAs shell, which is of great importance for applications [1]. In the present work, we use the fractal dimension method to explore polaron effects in GaAs/Al_xGa_{1-x}As core–shell nanowires.

The rest of this paper is organized as follows. The fractal dimension method of handling polaron effects in cylindrical GaAs/Al_xGa_{1-x}As core–shell nanowires is explained theoretically in Section 2. Numerical results and analyses are presented in Section 3. Finally, conclusions are drawn from this study in Section 4.

2 Model and theory

We consider a bound polaron in a cylindrical GaAs/Al_xGa_{1-x}As core–shell nanowire consisting of an Al_xGa_{1-x}As core ($0 \le r < r_1$) surrounded by a GaAs shell ($r_1 \le r < r_2$). Further, we suppose that no electron can escape from the structure. The confinement potential energy of the structure is described as

$$V(r) = \begin{cases} V_0, & 0 \le r \le r_1 \\ 0, & r_1 < r \le r_2 \\ \infty, & r > r_2 \end{cases}, \tag{1}$$

where V_0 is the band offset between the conduction bands of the core and shell materials with the shell width $r_w = r_2 - r_1$, and r is the radius in the cylindrical coordinate system. The GaAs/Al_xGa_{1-x}As material has a small electron–LO phonon coupling constant ($\alpha \ll 1$), and we will explore the case of weak coupling. The model of the GaAs/Al_xGa_{1-x}As core–shell nanowire and band alignment are shown in Fig. 1.

Under the effective mass approximation, we write the Schrödinger equation of the system as

$$H_{3D}\psi_{3D}(\boldsymbol{r}) = E_{3D}(\boldsymbol{r})\psi_{3D}(\boldsymbol{r}). \tag{2}$$

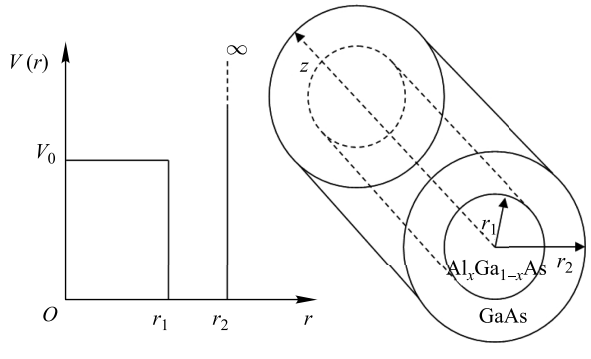

Fig. 1 Model of GaAs/Al_xGa_{1-x}As core–shell nanowire and band alignment.

Here, H_{3D} is the effective mass Hamiltonian,

$$H_{3D} = \frac{1}{2}P\frac{1}{m_i}P + V(\boldsymbol{r}), \tag{3}$$

where $P = -i\hbar\nabla$ is the canonical momentum operator, and m_i represents the electron effective mass. Note that

$$m_i = \begin{cases} m_1, & 0 \le r \le r_1 \\ m_2, & r_1 < r \le r_2 \end{cases}. \tag{4}$$

In a cylindrical core–shell nanowire grown along the z direction, the corresponding eigenfunction has the form

$$\psi_{3D}(\boldsymbol{r}) = Ce^{ik_z z}\psi_{2D}(r,\varphi), \tag{5}$$

where C = const, φ is the polar angle, and k_z is a quantum number representing the translational symmetry along the z direction. This form reduces the complexity of the eigenvalue problem to two coordinates, r and φ,

$$H_{2D}\psi_{2D}(r,\phi) = E\psi_{2D}(r,\phi), \tag{6}$$

where

$$H_{2D} = -\frac{\hbar^2}{2}\left[\frac{1}{r}\frac{\partial}{\partial r}\left(\frac{r}{m_i}\frac{\partial}{\partial r}\right) + \frac{1}{m_i}\frac{1}{r^2}\frac{\partial^2}{\partial\phi^2}\right] + V(r). \tag{7}$$

Moreover, we can further reduce the complexity by using axial symmetry

$$\psi_{2D}(r,\phi) = \frac{1}{\sqrt{2\pi}}e^{il\phi}\psi(r), \tag{8}$$

where l is the orbital quantum number. The Schrödinger equation for ψ is then

$$\left[\frac{1}{r}\frac{d}{dr}\left(\frac{r}{m_i}\frac{d\psi(r)}{dr}\right) - \frac{l^2\psi(r)}{m_i r^2}\right] + \left[V(r) + \frac{\hbar^2 k_z^2}{2m}\right]\psi(r) = E\psi(r). \tag{9}$$

As the computation of the $k_z \neq 0$ states does not result in any qualitative difference in the obtained results, we consider only the case $k_z = 0$. The Schrödinger equation then becomes

$$\left[\frac{1}{m_i}\frac{d^2\psi(r)}{dr^2} + \frac{1}{m_i}\frac{1}{r}\frac{d\psi(r)}{dr} + \frac{d}{dr}\left(\frac{1}{m_i}\right)\frac{d\psi(r)}{dr} - \frac{l^2\psi(r)}{m_i r^2}\right] + V(r)\psi(r) = E\psi(r). \tag{10}$$

Within the framework of the effective mass approximation, $\psi(r)$ satisfying the Schrödinger equation (10) is a linear combination of the Bessel function of the first kind, Bessel function of the second kind, modified Bessel function of the first kind, and modified Bessel function of the second kind.

Following the fractal dimension method, we can convert a polaron confined in the actual low-dimensional

structure into a free polaron in a fractal dimension system. The polaron corrections in the fractal dimension can be calculated according to second-order perturbation theory. The polaron energy shift is [7–10]

$$\Delta E = \alpha\hbar\omega_{LO}G_1(D); \tag{11}$$

In addition, we have the effective mass of the polaron [7–10]:

$$m^* = \frac{m}{1-\alpha G_2(D)}. \tag{12}$$

In Eqs. (11) and (12), ω_{LO} refers to the LO phonon limiting frequency approximation without dispersive effects, D represents the fractal dimension, α is the Fröhlich constant, m is the effective mass of electrons, and the functions $G_1(D)$ and $G_2(D)$ are obtained from

$$G_1(D) = \frac{\sqrt{\pi}}{2}\frac{\Gamma[(D-1)/2]}{\Gamma[D/2]} \tag{13}$$

and

$$G_2(D) = \frac{\sqrt{\pi}}{4}\frac{\Gamma[(D-1)/2]}{D\Gamma[D/2]}. \tag{14}$$

In Eqs. (13) and (14), $\Gamma(x)$ refers to the gamma function. The fractal dimensionality of our system is determined from [7–10]

$$D = 3 - 2\exp\left(\frac{L_w^*}{2R_p}\right), \tag{15}$$

where L_w^* is the effective length of quantum confinement, and $R_p = \sqrt{\hbar/2m\omega_{LO}}$ is the radius of the polaron. For our system, the effective length has the form

$$L_w^* = 2(r_w + \frac{1}{k_1}), \tag{16}$$

where k_1 refers to the electron wave vector in the core and can be obtained from the relation

$$k_1 = \frac{\sqrt{2m_1(V_0 - E)}}{\hbar}. \tag{17}$$

The ground state eigenenergy E of the electron is then obtained by solving the Schrödinger equation (10).

In a cylindrical GaAs/Al_xGa_{1-x}As core–shell nanowire, the material parameters characterizing the polaron properties in the core are different from those in the shell. Taking into account this problem, we introduce the method of averaging the parameters over all the effective fractal dimension regions. The average parameter values of the material that characterize the fractal dimension electron–phonon interaction have the forms [9]

$$m^{-1} = \sum_{i=1,2}\frac{P_i}{m_i}, \tag{18}$$

$$\omega_{LO} = \sum_{i=1,2}\omega_i P_i, \tag{19}$$

$$\alpha = \left[\sum_{i=1,2}\left(P_i\frac{\omega_i}{\omega_{LO}}\sqrt{\alpha_i\sqrt{\frac{m\omega_{LO}}{m_i\omega_i}}}\right)\right]^2, \tag{20}$$

$$R_p = \left[\sum_{i=1,2}\left(P_i\frac{\omega_i}{\omega_{LO}}\sqrt{\frac{\alpha_i R_{pi}}{\alpha}}\right)\right]^2, \tag{21}$$

$$R_{pi} = \sqrt{\frac{\hbar}{2m_i\omega_i}}. \tag{22}$$

In Eqs. (18)–(22), ω_i represent the phonon frequencies, α_i are the Fröhlich constants in different regions, and

$$P_1 = \int_0^{r_1}|\psi(r)|^2 dr, \tag{23}$$

$$P_2 = 1 - P_1 \tag{24}$$

represent the chances of the electron appearing in the core ($Al_xGa_{1-x}As$) and shell (GaAs) regions. The bound polaron binding energy and mass shift in the GaAs shell of the cylindrical GaAs/Al_xGa_{1-x}As core–shell nanowire can then be calculated quickly and simply according to Eqs. (11), (12), and (15). Using the average material parameters given by Eqs. (18)–(24), the corresponding shell-width-dependent polaron properties are calculated.

3 Numerical results and analyses

Figure 2 shows the calculated polaron binding energies as a function of shell width in the GaAs/Al_xGa_{1-x}As core–shell nanowire for different Al contents at a given core radius, $r_1 = 20$ Å. The data show that the numerical value

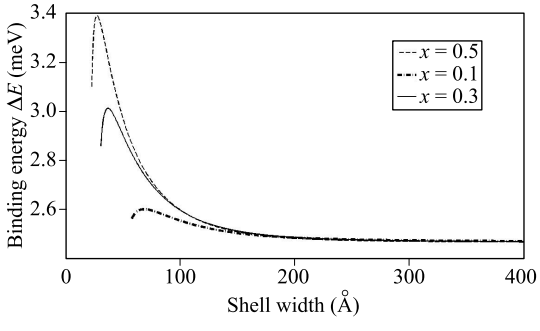

Fig. 2 Polaron binding energy as a function of shell width in GaAs/Al_xGa_{1-x}As core–shell nanowires at core radius $r_1 = 20$ Å.

of the binding energy first increases at different Al contents as the shell width r_w increases and then decreases monotonously as the shell width continues to increase. For a very large shell width, the polaron binding energy stays constant over the entire range. The maximum values appear at the $Al_xGa_{1-x}As$ shell width $r_w = 27.5$ Å for $x = 0.5$, $r_w = 37$ Å for $x = 0.3$, and $r_w = 67$ Å for $x = 0.1$. Figure 3 shows the shell width dependence of the polaron mass shift, $m = (m^* - m)/(m_2^* - m_2)$. Note that, for a narrow shell width, the Al content obviously affects the polaron binding energy and mass shift, which decrease with decreasing aluminum content. However, the aluminum content does not significantly influence them at a large shell width.

Figures 2 and 3 show that the polaron binding energy and mass shift in the GaAs shell first increase with increasing shell width, reach their maximum values, and then decrease. Note that this behavior is predicted by research on a polaron confined in a finite-potential quantum wire [14].

Figure 4 shows the fractal dimension D as a function of shell width for the nanowires described in Figs. 2 and 3. In Fig. 4, we see that the cylindrical $GaAs/Al_xGa_{1-x}As$ core–shell nanowire behaves as a large block for a very large shell width. Accordingly, the dimension has the maximum value, $D = 3$. This system becomes increasingly squeezed as the shell width decreases. Consequently, the polaron becomes increasingly confined. Further, the acting dimension decreases, reaching a minimum at the shell width $r_w = 30.5$ Å for $x = 0.5$, $r_w = 36$ Å for $x = 0.3$, and $r_w = 68$ Å for $x = 0.1$. Then the dimension increases as the shell width decreases further. We can intuitively understand that the fractal dimension first decreases when the shell width decreases for a large shell width because the main polaron wave function is constrained inside the shell. The fractal dimension will increase when the shell width becomes small enough for polaron tunneling into the core. The fractal dimension method provides an appropriate technique that is simple and applicable to the GaAs/AlGaAs core–shell nanowire system.

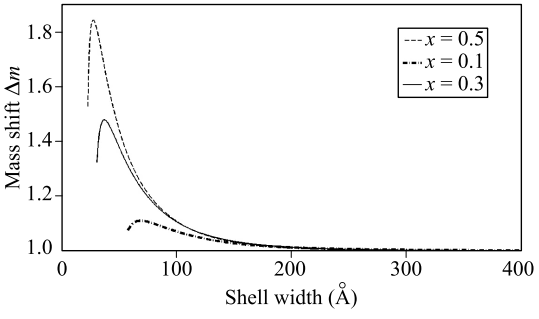

Fig. 3 Polaron mass shift as a function of shell width in $GaAs/Al_xGa_{1-x}As$ core–shell nanowires at core radius $r_1 = 20$ Å.

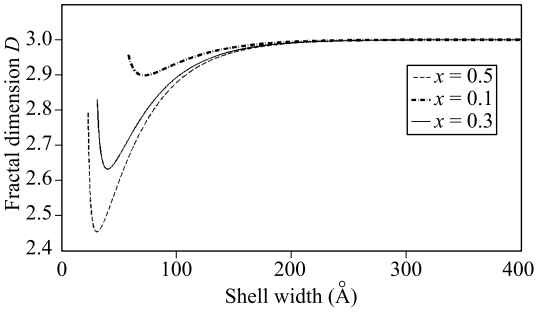

Fig. 4 Fractal dimension as a function of shell width for a polaron in $GaAs/Al_xGa_{1-x}As$ core–shell nanowires at core radius $r_1 = 20$ Å.

In Figs. 2–4, we see that the peaks of the polaron binding energy and mass shift and the minimum position of the fractal dimension decrease with increasing Al content in the core. The polaron binding energy and mass shift increase as the Al content increases at a narrow shell width. In contrast, the fractional dimension decreases. For a very large shell width, the Al content does not affect the physical characteristics in Figs. 2–4 because the fractal dimension tends to be 3 when the shell width becomes very large. Consequently, the polaron binding energy and mass shift tend to have their 3D GaAs bulk values [8].

In our previous work, we studied polaron effects in $GaAs/Al_xGa_{1-x}As$ thin films [10]. Compared with that of a polaron in a $GaAs/Al_xGa_{1-x}As$ thin film, the fractal dimension of a polaron in a $GaAs/Al_xGa_{1-x}As$ core–shell nanowire is slightly higher for the same Al content, $x = 0.3$. This is because the $GaAs/Al_xGa_{1-x}As$ core–shell nanowire system doubles the quantum well width, and polarons can tunnel into the core at different polar angles. Note that the $GaAs/Al_xGa_{1-x}As$ core–shell nanowire is widely regarded as an important quasi-one-dimensional structure for experiments, although the core–shell nanowire size often used in experiments actually provides quasi-two-dimensional confinement of a polaron. However, compared with that in the $GaAs/Al_xGa_{1-x}As$ thin film, the polaron binding energy in the $GaAs/Al_xGa_{1-x}As$ core–shell nanowire is slightly lower for the same Al content, $x = 0.3$. This is because the higher fractal dimension leads to less confinement. Polaron problems in heterostructures are very complicated owing to the presence of a variety of phonon modes such as bulklike phonons, interface phonons, half-space phonons, and slab phonons. By using the fractal dimension method, polaron corrections in different morphological systems can be calculated by considering only one bulk phonon mode and the dimension.

Further, to explain the pattern of changes in the

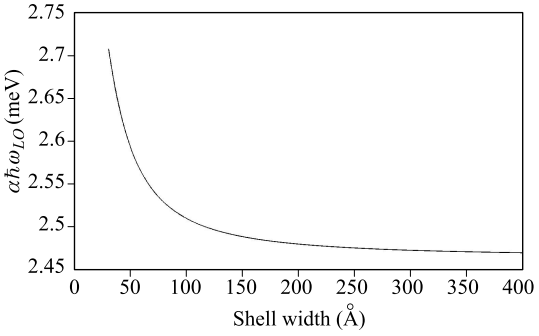

Fig. 5 Determinant $\alpha\hbar\omega_{LO}$ as a function of shell width in GaAs/Al_xGa_{1-x}As core–shell nanowire with $x = 0.3$ at core radius $r_1 = 20$ Å.

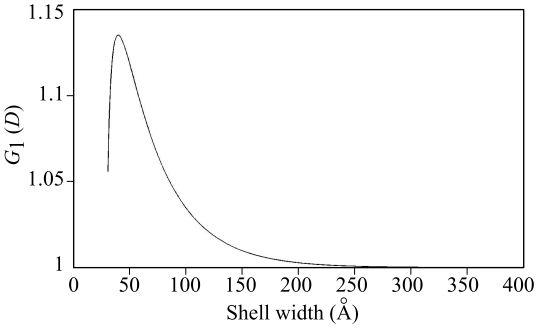

Fig. 6 Determinant $G_1(D)$ as a function of shell width in GaAs/Al_xGa_{1-x}As cor–shell nanowires with $x = 0.3$ at the core radius $r_1 = 20$ Å.

polaron binding energy clearly, we consider the determinants $\alpha\hbar\omega_{LO}$ and $G_1(D)$. Analysis of the pattern of the polaron mass shift is similar to that of the polaron binding energy, and we omit it. According to Eq. (11), the polaron binding energy is determined by the determinants $\alpha\hbar\omega_{LO}$ and $G_1(D)$. The former is influenced by the chance that an electron will appear in different regions and the material parameters. The latter is influenced by the system dimension. In Figs. 5 and 6, we take the Al content $x = 0.3$ as an example. A comparison of Figs. 5 and 6 shows that for a large shell width, $r_w > 40$ Å, both $\alpha\hbar\omega_{LO}$ and $G_1(D)$ increase with decreasing shell width. Thus, the polaron binding energy is increased by decreasing the shell width in the region $r_w > 40$ Å. When $r_w \leq 40$ Å, the determinant $\alpha\hbar\omega_{LO}$ continues to increase with decreasing shell width. On the other hand, the determinant $G_1(D)$ starts to decrease with decreasing shell width in this range. This is because the relationship with the fractal dimension D changes. For a large shell width, the effective length of quantum confinement will decrease with decreasing shell width. When the shell width becomes small enough, the effective length of quantum confinement starts to decrease for polaron tunneling into the core. As shown in equation (14), this will change the relationship with the fractal dimension directly. In the region 37 Å $\leq r_w \leq$ 40 Å, the determinant $\alpha\hbar\omega_{LO}$ increases more rapidly than $G_1(D)$ decreases with decreasing shell width. Consequently, the polaron binding energy continues to increase with decreasing shell width in this region and reaches a peak value at the shell width $r_w = 40$ Å. In the region $r_w < 40$ Å, just the opposite occurs; the determinant $G_1(D)$ decreases more quickly, and the polaron binding energy finally begins to decrease.

The relationship between the shell width and the polaron binding energy in the GaAs shell for $Al_{0.3}Ga_{0.7}As$ at core radii $r_1 = 40$, 90, and 140 Å is shown in Fig. 7. The shell width versus the polaron mass shift is shown in Fig. 8. For different core radii, the curves of the polaron binding energy and mass shift also first increase as the shell width r_w increases. Then they decrease as the shell width continues to increase. For a very large shell width, the polaron binding energy remains constant over the entire range. The maximum values appear at $Al_xGa_{1-x}As$ shell widths of $r_w = 33$ Å for $r_1 = 40$ Å, $r_w = 33$ Å for $r_1 = 90$ Å, and $r_w = 35$ Å for $r_1 = 40$ Å. From Figs. 7 and 8, we notice that the polaron binding energy and mass shift decrease as the core radius decreases. Remarkably, for a narrow shell width, the core radius has a meaningful effect on the polaron binding energy and

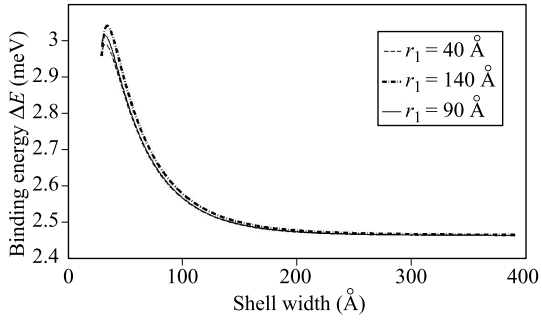

Fig. 7 Polaron binding energy as a function of shell width in GaAs/$Al_{0.3}Ga_{0.7}$ core–shell nanowires at core radii $r_1 =$ 40, 90, and 140 Å.

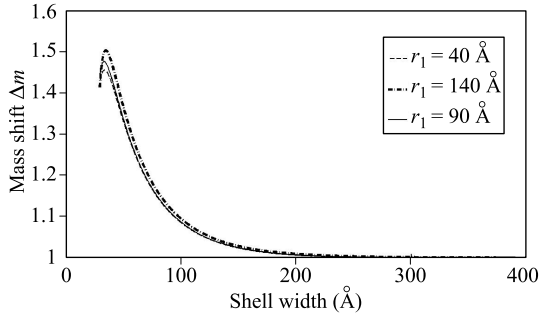

Fig. 8 Polaron mass shift as a function of shell width in GaAs/$Al_{0.3}Ga_{0.7}As$ core–shell nanowires at core radii $r_1 =$ 10, 20, and 30 Å.

mass shift, which decrease as the core radius decreases. However, the core radius does not significantly influence them for a large shell width.

Figure 9 shows plots of the fractal dimension D versus shell width for the core radius values in Figs. 7 and 8. We see that the cylindrical GaAs/Al_xGa_{1-x}As core–shell nanowire behaves as a large block for a very large shell width. The dimension has its maximum value, $D = 3$. The effective dimension first drops as the shell width decreases, reaches a minimum, and then increases as the shell width continues to decrease. The data in Fig. 9 show that in a certain range, the core radius does not greatly affect the fractional dimension, as the main polaron wave function is constrained inside the shell.

4 Conclusions

We present for the first time the polaron binding energy and mass shift in GaAs/Al_xGa_{1-x}As core–shell nanowires. We use the fractal dimension method, which considers the GaAs/Al_xGa_{1-x}As core–shell nanowire as an effective fractal dimension system. In this system, the polaron is assumed to be unconfined. The fractal dimension measures the extent of confinement in the real environment. Here, the polaron properties of GaAs/Al_xGa_{1-x}As core–shell nanowires with different core radii and aluminum concentrations are studied. The fractal dimension method allows measurement of the polaron properties, such as the polaron binding energy and mass shift, in a simple analytical way, avoiding the complex calculations needed in traditional methods. In this article, the effects of the shell width on the polaron binding energy and mass shift are obtained for GaAs/Al_xGa_{1-x}As core–shell nanowires. The results show that both the polaron binding energy and mass shift first increase as the shell width increases, reach maximum values, and then decrease as the shell width of the GaAs/Al_xGa_{1-x}As core–shell nanowires continues to increase. Our calculations provide some reference values for varying the optical and electronic properties, which are important properties of GaAs/Al_xGa_{1-x}As core–shell nanowires, by changing the shell width [23].

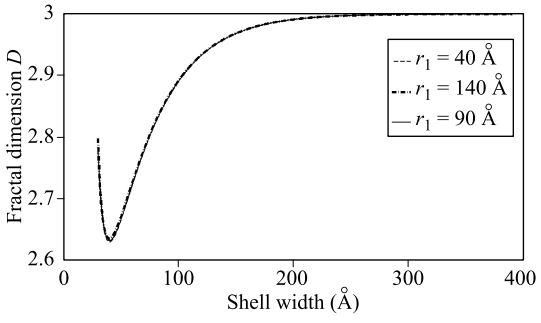

Fig. 9 Calculated fractal dimension as a function of shell width for a polaron in GaAs/$Al_{0.3}Ga_{0.7}$As core–shell nanowires at core radii $r_1 = 40$, 90, and 140 Å.

References

1. B. Mayer, D. Rudolph, J. Schnell, S. Morkötter, J. Winnerl, J. Treu, K. Müller, G. Bracher, G. Abstreiter, G. Koblmüller, and J. J. Finley, Lasing from individual GaAs-AlGaAs core–shell nanowires up to room temperature, *Nat. Commun.* 4, 2931 (2013)
2. A. Lubk, D. Wolf, P. Prete, N. Lovergine, T. Niermann, S. Sturm, and H. Lichte, Nanometer-scale tomographic reconstruction of three-dimensional electrostatic potentials in GaAs/AlGaAs core–shell nanowires, *Phys. Rev. B* 90(12), 125404 (2014)
3. S. Morkötter, N. Jeon, D. Rudolph, B. Loitsch, D. Spirkoska, E. Hoffmann, M. Döblinger, S. Matich, J. J. Finley, L. J. Lauhon, G. Abstreiter, and G. Koblmüller, Demonstration of confined electron gas and steep-slope behavior in delta-doped GaAs-AlGaAs core–shell nanowire transistors, *Nano Lett.* 15(5), 3295 (2015)
4. N. Jiang, P. Parkinson, Q. Gao, S. Breuer, H. H. Tan, J. Wong-Leung, and C. Jagadish, Long minority carrier lifetime in Au-catalyzed GaAs/Al_xGa_{1-x}As core-shell nanowires, *Appl. Phys. Lett.* 101(2), 023111 (2012)
5. D. Rudolph, S. Funk, M. Döblinger, S. Morkötter, S. Hertenberger, L. Schweickert, J. Becker, S. Matich, M. Bichler, D. Spirkoska, I. Zardo, J. J. Finley, G. Abstreiter, and G. Koblmüller, Spontaneous alloy composition ordering in GaAs-AlGaAs core–shell nanowires, *Nano Lett.* 13(4), 1522 (2013)
6. X. F. He, Excitons in anisotropic solids: The model of fractional-dimensional space, *Phys. Rev. B* 43(3), 2063 (1991)
7. A. Matos-Abiague, A fractional-dimensional space approach to the polaron effect in quantum wells, *J. Phys. Condens. Matter* 14(17), 4543 (2002)
8. A. Matos-Abiague, Fractional-dimensional space approach for parabolic-confined polarons, *Semicond. Sci. Technol.* 17(2), 150 (2002)
9. A. Matos-Abiague, Polaron effect in GaAs-$Ga_{1-x}Al_x$As quantum wells: A fractional-dimensional space approach, *Phys. Rev. B* 65(16), 165321 (2002)
10. Z. H. Wu, H. Li, L. X. Yan, B. C. Liu, and Q. Tian, Fractional-dimensional space approach for the polaron in a GaAs film deposited on Al_xGa_{1-x}As substrate, *Physica B* 410, 28 (2013)
11. Z. H. Wu, H. Li, L. X. Yan, B. C. Liu, and Q. Tian, The polaron in a GaAs film deposited on Al_xGa_{1-x}As influenced by the thickness of the Substrate, *Superlattices Microstruct.* 55, 16 (2013)

12. H. Li, B. C. Liu, B. X. Shi, S. Y. Dong, and Q. Tian, Novel method to determine effective length of quantum confinement using fractional-dimension space approach, *Front. Phys.* 10(4), 107302 (2015)

13. Z. H. Wu, L. Chen, and Q. Tian, Exciton binding energies in GaAs films on $Al_xGa_{1-x}As$ substrates, *Int. J. Mod. Phys. B* 29(30), 1550213 (2015)

14. A. L. Vartanian, A. L. Asatryan, and L. A. Vardanyan, Influence of both electric and magnetic fields on the polaron properties in a finite-potential quantum well wire, *Physica E* 47, 134 (2013)

15. P. Christol, P. Lefebvre and H. Mathieu, Fractional-dimensional calculation of exciton binding energies in semiconductor quantum wells and quantum-well wires, *J. Appl. Phys.* 74(9), 5626 (1993)

16. P. Lefebvre, P. Christol, and H. Mathieu, Excitons in semiconductor superlattices: Heuristic description of the transfer between Wannier-like and Frenkel-like regimes, *Phys. Rev. B* 46(20), 13603 (1992)

17. A. Thilagam and A. Matos-Abiague, Excitonic polarons in confined systems, *J. Phys.: Condens. Matter* 16(23), 3981 (2004)

18. E. Reyes-Gómez, L. E. Oliveira, and M. de Dios-Leyva, Shallow impurities in semiconductor superlattices: A fractional-dimensional space approach, *J. Appl. Phys.* 85(8), 4045 (1999)

19. I. D. Mikhailov, F. J. Betancur, R. A. Escorcia, and J. Sierra-Ortega, Shallow donors in semiconductor heterostructures: Fractal dimension approach and the variational principle, *Phys. Rev. B* 67(11), 115317 (2003)

20. J. Kundrotas, A. Čerškus, S. Ašmontas, G. Valušis, B. Sherliker, M. P. Halsall, M. J. Steer, E. Johannessen, and P. Harrison, Excitonic and impurity-related optical transitions in Be_δ-doped GaAs/AlAs multiple quantum wells: Fractional-dimensional space approach, *Phys. Rev. B* 72(23), 235322 (2005)

21. J. Kundrotas, A. Cerškus, S. Ašmontas, G. Valušis, M. P. Halsall, E. Johannessen, and P. Harrison, Impurity-induced Huang–Rhys factor in Be_δ-doped GaAs/AlAs multiple quantum wells: Fractional-dimensional space approach, *Semicond. Sci. Technol.* 22(9), 1070 (2007)

22. M. A. Smondyrev, B. Gerlach, and M. O. Dzero, Mean parameter model for the Pekar–Fröhlich polaron in a multilayered heterostructure, *Phys. Rev. B* 62(24), 16692 (2000)

23. M. Hocevar, L. T. Thanh Giang, R. Songmuang, M. den Hertog, L. Besombes, J. Bleuse, Y.M. Niquet, and N. T. Pelekanos, Residual strain and piezoelectric effects in passivated GaAs/AlGaAs core-shell nanowires, *Appl. Phys. Lett.* 102(19), 191103 (2013)